Variations of the tropical Atlantic and Pacific SSS minimum zones and their relations to the ITCZ and SPCZ rain bands (1979-2009)

Michel Tchilibou, Thierry Delcroix, Gaël Alory, Sabine Arnault, Gilles Reverdin

AGU PUBLICATIONS

JGR

Journal of Geophysical Research: Oceans

RESEARCH ARTICLE

10.1002/2015JC010836

Key Points:
- Low SSS waters appear further poleward than ITCZ/SPCZ E-P minima
- Low SSS waters and E-P minima migrate at seasonal and interannual time scales
- Long-term (1979–2009) meridional migrations appear more clearly in the SPCZ

Correspondence to:
T. Delcroix,
Thierry.delcroix@ird.fr

Citation:
Tchilibou, M., T. Delcroix, G. Alory, S. Arnault, and G. Reverdin (2015), Variations of the tropical Atlantic and Pacific SSS minimum zones and their relations to the ITCZ and SPCZ rain bands (1979–2009), *J. Geophys. Res. Oceans*, *120*, 5090–5100, doi:10.1002/2015JC010836.

Received 11 MAR 2015
Accepted 5 JUN 2015
Accepted article online 13 JUN 2015
Published online 23 JUL 2015

Variations of the tropical Atlantic and Pacific SSS minimum zones and their relations to the ITCZ and SPCZ rain bands (1979–2009)

M. Tchilibou[1], T. Delcroix[2], G. Alory[1,2], S. Arnault[3], and G. Reverdin[3]

[1]Chaire Internationale en Physique Mathematique et Applications, UNESCO, Cotonou, Bénin, [2]Laboratoire d'Etudes en Géophysique et Océanographie Spatiale, Toulouse, France, [3]Laboratoire d'Océanographie et du Climat: Expérimentations et Approches Numériques, Paris, France

Abstract This study focuses on the time-space variability of the low Sea Surface Salinity (SSS) waters extending zonally within 2°N–12°N in the Atlantic and Pacific and within 6°S–16°S in the western third of the Pacific. The analysis is based on a combination of in situ SSS observations collected in the last three decades from voluntary observing ships, TAO/TRITON and PIRATA moorings, Argo floats, and (few) CTD profiles. The mean latitudes of the Atlantic and Pacific low SSS waters appear 1°–3° further poleward than the Evaporation minus Precipitation (E-P) minima linked to the Inter Tropical Convergence Zones (ITCZ) and South Pacific Convergence Zone (SPCZ). At the seasonal time scale, the E-P minima migrate poleward in summer hemispheres, leading the migration of the SSS minima by 2–3 months in the Atlantic ITCZ, Pacific SPCZ, and in the eastern part of the Pacific ITCZ. On the other hand, the seasonal displacements of E-P and SSS minima are in antiphase in the central and western parts of the Pacific ITCZ. At the interannual time scale, the E-P and SSS minima migrate poleward during La Nina events in the Pacific and during the positive phase of the Atlantic Meridional Dipole (AMD) in the Atlantic (and vice versa during El Nino and the negative phase of the AMD). We further document long-term (1979–2009) meridional migrations of the E-P and SSS minima, especially in the SPCZ region, and discuss whether or not they are consistent with documented SST and wind stress trends.

1. Introduction

Sea Surface Salinity (SSS) is an important variable of the Global Climate Observing System [*GCOS*, 2004]. It is recognized as an Essential Climate Variable (ECV) and its sustained in situ monitoring was strongly recommended in the outcomes of the Oceanobs09 international conference [see *Lagerloef et al*., 2010]. Its importance for climate has further motivated the recent advent of the dedicated SMOS and Aquarius satellite missions.

The overall scientific importance of studying changes in SSS is due to its role in changing seawater density (and thus density gradients). Horizontal and vertical gradients in density affect horizontal currents and mixed layer depths which are involved in climate relevant heat transport regulation and ocean-atmosphere interactions, respectively. In practice, SSS has been shown to be an inspiring ECV to analyze, at least to improve our understanding of river discharge effects close to and away from the coast, barrier layer formation, seasonal and interannual climate changes, ENSO (El Nino Southern Oscillation) main features, sea level changes, and marine water cycle changes in the context of paleo and global climate change studies [e.g., *Delcroix and Murtugudde*, 2002; *Boyer and Levitus*, 2002; *Bingham et al*., 2010; *Maes et al*., 2006; *Singh et al*., 2011; *Terray et al*., 2012; *Durack and Wijffels*, 2010; *Le Bec et al*., 2000].

As far as the marine water cycle is concerned, the spatial correspondence between the mean distributions of SSS and Evaporation minus Precipitation (E-P) has been pointed out in numerous papers [e.g., *Levitus*, 1986]. For instance, in the tropical Atlantic and Pacific oceans, the regions of interest here, the highest SSS values are found slightly poleward of where E-P reach maximum values close to the centers of large-scale subtropical gyres (see Figure 1). Similarly, the lowest SSS values are found where E-P reach minimum values roughly underneath regions commonly referred to as the Atlantic and Pacific ITCZ (Inter Tropical Convergence Zone),

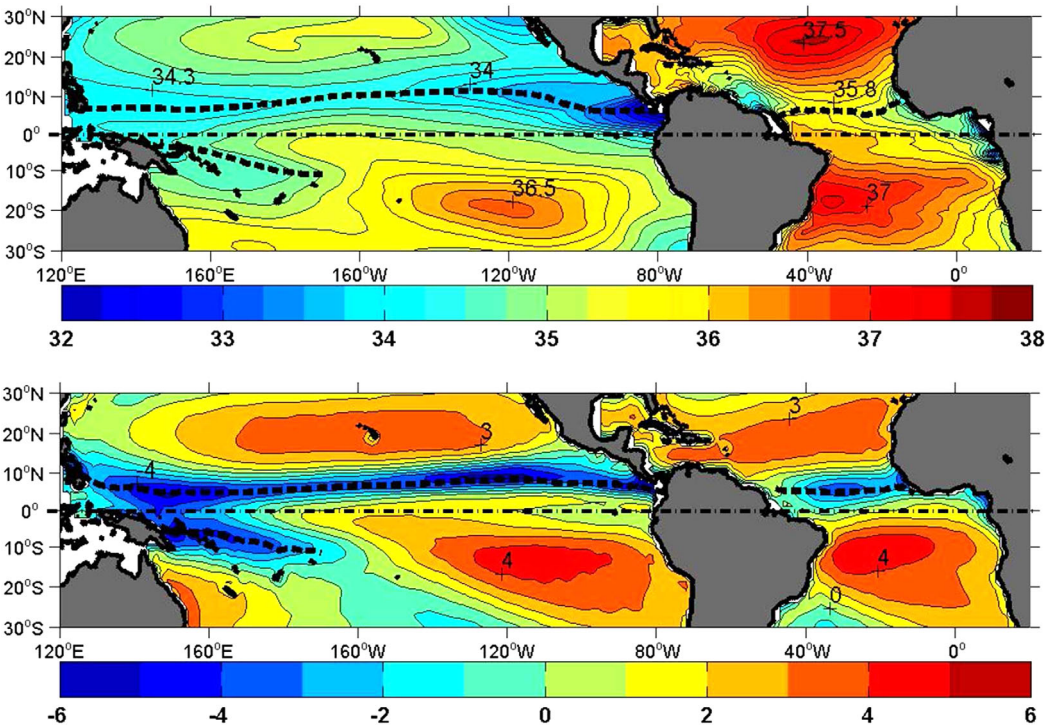

Figure 1. Spatial distribution of the 1979–2009 averaged (top) SSS (pss-1978) and (bottom) E-P budget (mm/d). The heavy dashed black lines denote the position of the (top) SSS and (bottom) E-P minimum values underneath the ITCZ and SPCZ. See section 2 for the data sources.

SPCZ (South Pacific Convergence Zone), and in the western Pacific warm pool, where moist winds converge and trigger atmospheric convection resulting in a band of heavy precipitation. Aside from this spatial correspondence, numerous studies have demonstrated connections between changes in SSS and E-P at the intraseasonal, seasonal, and interannual time scales and, more recently, on "long-term" trends. In that latter case, analyses of data collected during the last decades show a clear tendency for SSS to increase in regions where E dominates and to decrease in regions where P dominates, that is in high and low mean SSS regions, respectively [*Delcroix et al.*, 2007; *Cravatte et al.*, 2009; *Durack and Wijffels*, 2010; *Terray et al.*, 2012]. These long-term SSS trends have been interpreted as resulting from changes in the atmospheric water vapor content under global warming, in line with the Clausius-Clapeyron relationship and the so-called dry-get-drier and wet-get-wetter paradigms [see *Held and Soden*, 2006]. Along with these long-term trends, *Cravatte et al.* [2009] have shown an eastward migration and expansion of the low-SSS water surface located in the western Pacific warm pool, and *Hasson et al.* [2013a] a westward migration of the high-SSS water surface located in the south-eastern tropical Pacific in the last decades. The mechanisms responsible for these observed migrations and their possible connections to low-frequency changes in E-P are not clearly established.

As noted above and illustrated in Figure 1, the core regions of low-SSS waters in the tropical Atlantic and Pacific oceans are more or less aligned with the core regions of E-P minima (or P maxima) featuring the surface imprint of the ITCZ and SPCZ rain bands (see section 2 for the data sources). To date, few studies have investigated changes in the mean position of these SSS and E-P minima, their connection, and the extent to which migrations of the SSS minima can be used as a proxy for migrations of the convergence zones. These issues are important as: (a) slight ITCZ or SPCZ migrations can induce large hydroclimatic changes in island countries and continental regions bordering the tropical Atlantic and Pacific, (b) the regions of SSS minima are characterized by relatively thick barrier layers [*de Boyer Montégut et al.*, 2007; *Tanguy et al.*, 2010; *Kao and Lagerloef*, 2014] which are known to impact the regional heat and momentum transfers between the ocean and the atmosphere, (c) these regions are flanked on either side by well-marked SSS fronts that record the signature of Tropical Instability Waves (TIW) [*Lee et al.*, 2012, 2014]. Moreover, major uncertainties in E-P fields reside in the ITCZ and SPCZ, at least before the TRMM (Tropical Rainfall Measurement Mission) satellite, and documenting changes in the locations of the SSS minima might help us to identify how these

convergence zones vary with climate and in long-term trends [*Xie and Arkin*, 1997; *Yu and Weller*, 2007; *Bellucci et al*., 2010; *Tian and Peters-Lidard*, 2010]. The aim of this study is thus to document changes in the location of these regions at different time scales, to contribute to clarifying the covariability of the SSS and E-P minima, relying in particular on three decades of in situ SSS data (1979–2009) that sample the SSS variability particularly well. The study is organized as follows. Section 2 describes the data and data processing. Section 3 presents the mean structures, the seasonal and interannual variability and the long-term trends. The conclusion is given in section 4.

2. Data and Data Processing

The two main sources of data we used are the Atlantic (20°S–50°N; 1970–2013) and Pacific (30°S–30°N; 1950–2009) SSS gridded products described in *Reverdin et al*. [2007] and *Delcroix et al*. [2011], respectively. These 1° × 1° × 1° month gridded products are based on an objective analysis of irregularly distributed in situ SSS data, originating mainly from Voluntary Observing Ships (VOS), TAO, TRITON, and PIRATA moorings, Argo floats (since 2004), and few cruise-derived CTD casts. The 1979–2009 Atlantic and Pacific common time period only will be investigated here given the time/space SSS data distribution and the related objective analysis error fields (not shown here).

We used the Global Precipitation Climatology Project (GPCP) data for P [*Adler et al*., 2003] and the OAFlux data for E [*Yu and Weller*, 2007] to build a 1° × 1° × 1° month E-P product covering the 1979–2009 years. These E and P products were selected as they have been suggested to be the best available products among roughly a dozen products for those years, based on comparisons with independent estimates [*Schanze et al*., 2010]. Two simple climate mode indices have been used: the Southern Oscillation Index (SOI) to characterize the El Niño and La Niña periods, and the Atlantic Meridional Dipole (AMD) index following the definition of *Servain et al*. [1999] using Sea Surface Temperature (SST) derived from the TropFlux data set [*Praveen Kumar et al*., 2012]. Specifically, the AMD index was computed as the difference in SST between the Atlantic 30°N–5°N and 5°N–20°S regions. (Note that we also used the Pacific Decadal Oscillation (PDO), the North Atlantic Oscillation (NAO), and the Atlantic Equatorial Mode (AEM) indices to characterize climate changes for the Pacific and Atlantic oceans. These indices are not presented here as they proved to be less correlated than the SOI and AMD to the observed SSS and E-P anomalies discussed below). The wind data were derived from the European Center for Medium Range Weather Forecasts (ECMWF) ERA-interim reanalysis [*Dee et al*., 2011].

Using the above-noted gridded fields, the latitudes of the SSS and E-P minima (hereafter SSSmin, E-Pmin) were computed monthly, at each degree of longitude, from 140°E to 20°W using data within 0°N–15°N in the Atlantic and Pacific (i.e., bracketing the ITCZ) and from 140°E to 170°W using data within 0°S–20°S in the western Pacific (i.e., bracketing the SPCZ). We then computed the 1979–2009 climatological means, standard deviations, and probability density functions of the SSSmin and E-Pmin latitudes. The spatiotemporal variability of SSSmin and E-Pmin can be examined in many different ways [e.g., *Bretherton et al*., 1992], and we chose to present single EOF analysis for the sake of simplicity. The EOF analyses were performed on the linearly detrended time series. As the resulting first EOF time functions (not shown here) included both seasonal and interannual variability, we then separated the original monthly time series into high (i.e., with periods equal or less than 12 months) and low (i.e., with periods greater than 12 months) frequency signal using a 25 month Hanning filter. EOF analyses were then performed separately on the low-pass and high-pass filtered time series. Note that values west of the international dateline were not considered when performing the EOF analysis on low-pass filtered time series, as the E-Pmin and SSSmin values were hardly identifiable due to a strong regional rearrangement of convection during El Niño events. Only the first EOF modes are presented here as no simple physical explanations were found to account for most of the other modes. A simple test of significance [*North et al*., 1982] applied to the eigenvalues shows that higher-order modes probably do not represent real physical phenomena. Linear trends were finally computed over the 1979–2009 years.

3. Results

3.1. Mean Structures

The 1979–2009 averaged latitudes of SSSmin and E-Pmin located underneath the ITCZ and SPCZ regions are shown in Figure 2 (top). In the Northern Hemisphere, the Pacific SSSmin stretches within 6°N–12°N

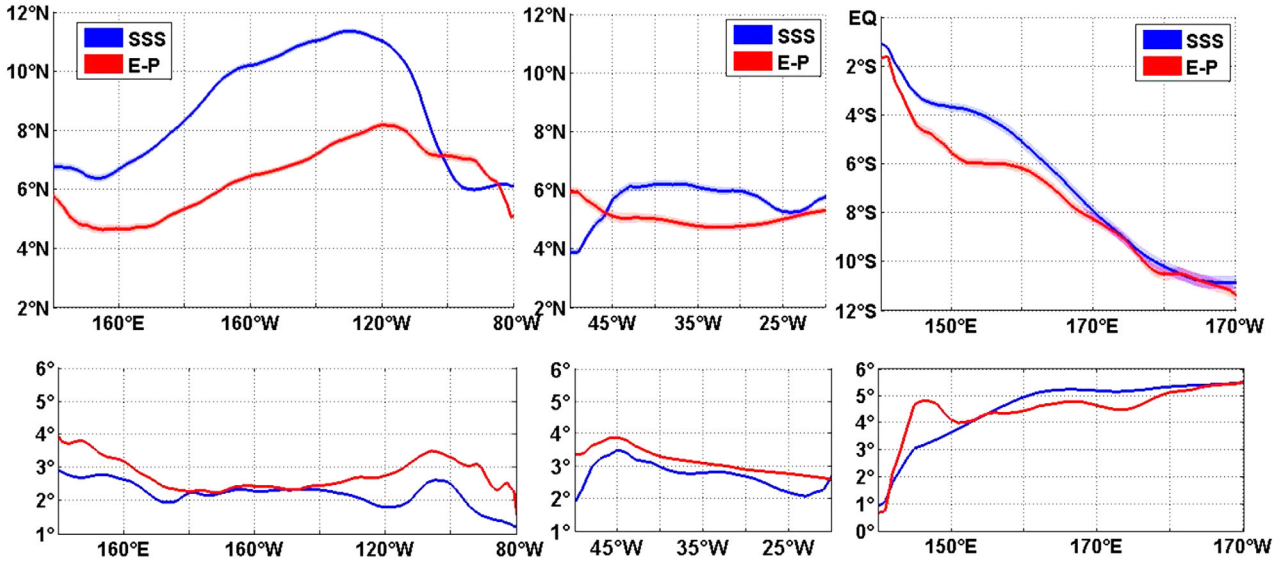

Figure 2. (top) Mean and (bottom) standard deviation of the latitudes of SSS (in blue) and E-P (in red) minimum values as a function of longitudes in the so-called (from left to right) Pacific-ITCZ, Atlantic-ITCZ, and Pacific-SPCZ regions. Values were computed from monthly time series covering the 1979–2009 years. A 5° longitude running mean was applied for clarity.

(reaching its northernmost position near 130°W), the Atlantic SSSmin within 4°N–6°N, and they are both located 1°–3° latitude to the north of the corresponding E-Pmin (except east of 100°W and west of 45°W). In the Southern Hemisphere, the Pacific SSSmin and E-Pmin are diagonally oriented from about 2°S–140°E to 11°S–170°W. These E-Pmin and SSSmin locations (based on 31 years of data) are in overall very good agreement with values derived from shorter time series of highly reflective clouds, SSS transoceanic VOS observations, precipitation-based estimates, and Aquarius SSS data [*Waliser and Gautier*, 1993; *Delcroix and Hénin*, 1991; *Delcroix et al*., 2005; *Vincent et al*., 2011; *Yu*, 2014]. The shifts in latitude between SSSmin and E-Pmin results mostly from the meridional Ekman salt transport linked to the trade winds at the ITCZ mean positions [e.g., *Delcroix and Hénin*, 1991].

The 1979–2009 standard deviations of SSSmin and E-Pmin latitudes (Figure 2, bottom) are of the order of 2°–4° for the ITCZ, slightly increasing from the east to the west, and 1°–5° for the SPCZ, increasing from the west to the east. Notable latitudinal changes are thus observed relative to the mean values. To further analyze these changes, we also computed the probability density functions of the latitudes of SSSmin and E-Pmin for all longitudes. As representative examples, Figure 3 shows three SSSmin and E-Pmin histograms calculated in 10° longitude bands with high data density centered at 160°E in the Pacific ITCZ, 30°W in the Atlantic ITCZ, and 170°E in the Pacific SPCZ. In agreement with Figure 2, these histograms confirm the overall tendency for SSSmin latitudes to be located slightly to the north of E-Pmin latitudes in the Atlantic and Pacific ITCZ regions. The SSSmin histograms are moderately Gaussian, and the differences between mean and median values (a common skewness indicator) are 13, 0.4, and 16% of the standard deviations, respectively. It is interesting to note that the SSS Atlantic histogram has a somewhat bimodal distribution with one peak at 3°N–4°N and the other at 7°N. Such a bimodality, not visible below on the EOF time function, mostly reflects the tendency for the SSS minimum values to be trapped near the southernmost latitude in spring and summer and then near the northernmost latitude in fall and winter, with a rapid latitudinal shift in between [see *Delcroix et al*., 2005, Figure 6]. Although not clearly visible on the E-Pmin histogram, this SSSmin shift could correspond to the abrupt ITCZ shift (bringing monsoon rains to the Sahel region) detected over West Africa [*Sultan and Janicot*, 2000]. The northern Pacific SSS distribution (at 160°E) has a secondary peak that shows the equatorial warm pool get sometimes fresher than the ITCZ region.

3.2. Seasonal Variability

The first seasonal EOF modes of SSSmin and E-Pmin latitudes shown in Figure 4 account for at least 2/3 of the "high"- frequency variance (see all percentage values in Table 1). The mean seasonal range is of the order of 2°–6° latitude. In the Atlantic, the northernmost latitudes of SSSmin are reached by the end of boreal fall, lagging behind E-Pmin by 2–3 months. These results match those observed in earlier studies

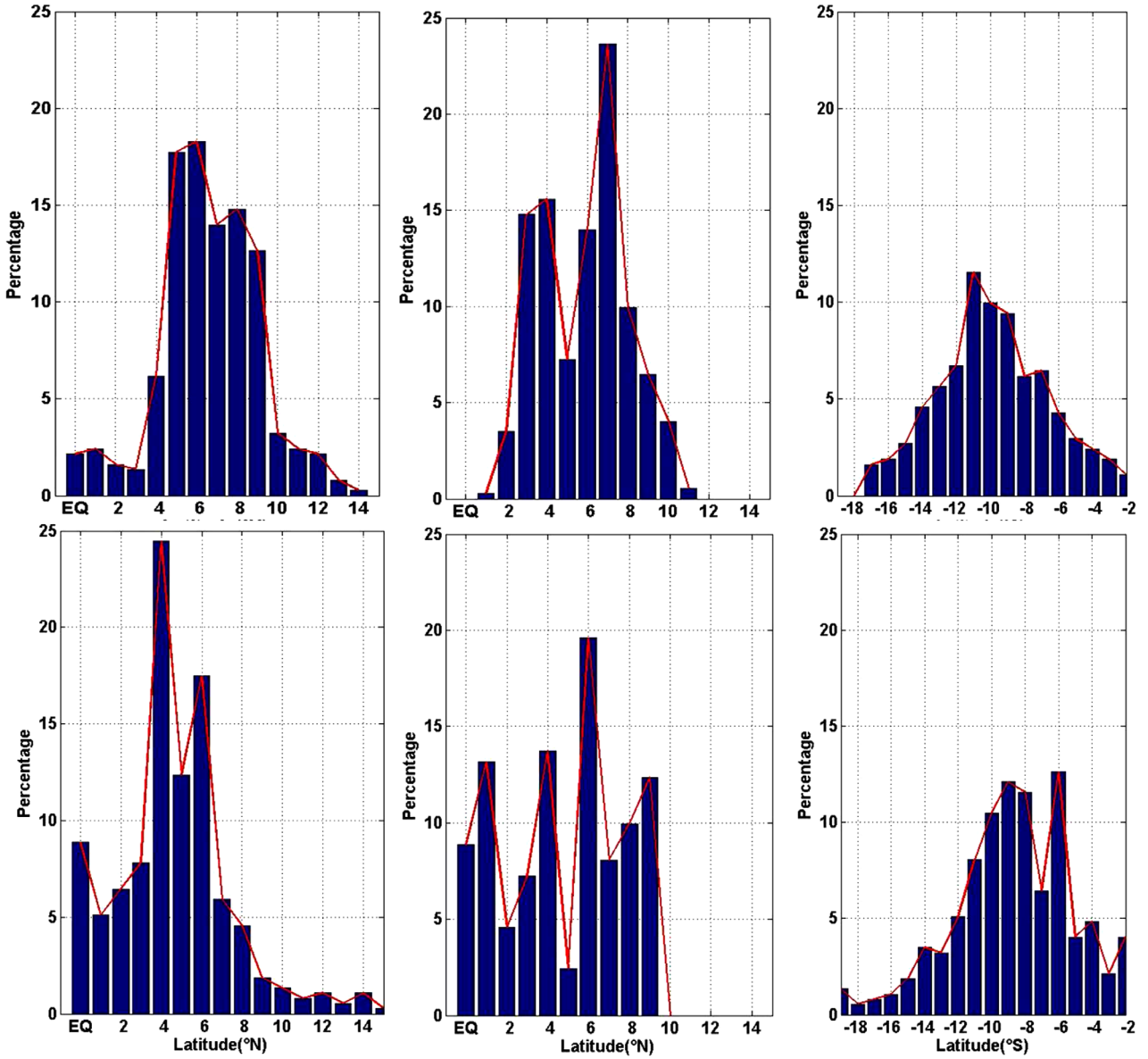

Figure 3. Probability density function of the latitudes of the (top) SSS and (bottom) E-P minimum values per 1° latitude bin, as averaged over 10° longitude bands centered (from left to right) at 160°E, 30°W, and 170°E in the so-called Pacific-ITCZ, Atlantic-ITCZ, and Pacific-SPCZ regions.

based on a subset of our SSS data [*Dessier and Donguy*, 1994], on recent Aquarius SSS data analyses [*Grodsky et al*., 2014; *Foltz et al*., 2015], and on different ITCZ definitions [*Citeau et al*., 1988; *Servain et al*., 2014]. A similar phasing for the seasonal migrations of SSSmin occurs in the eastern part only (east of 110°W) of the Pacific ITCZ. In the SPCZ region, the southernmost latitudes of SSSmin are reached by the end of austral summer, still lagging behind E-Pmin by 2–3 months. This 2–3 month time lag (about a quarter of an annual cycle) is expected if variations of SSS were governed only by a sinusoidal annual variation of E-P [see *Hires and Montgomery*, 1972; *Delcroix and Hénin*, 1991]. Surprisingly, when compared with the above-analyzed regions, the seasonal migrations of SSSmin and E-Pmin are in antiphase in the central and western parts of the Pacific ITCZ (west of 110°W). Specifically, SSSmin moves south of its mean latitude while E-Pmin moves north of its mean latitude in the second half of the year, and vice versa in the first half of the year. This peculiarity, which also shows up in the analysis of 2 years of Aquarius data, was discussed by *Yu* [2014]. In a more complete analysis, *Yu* [2015] computed all terms of the mixed-layer salinity equation and concluded that the seasonal migration of the salinity front associated with SSSmin is dominated by Ekman dynamics

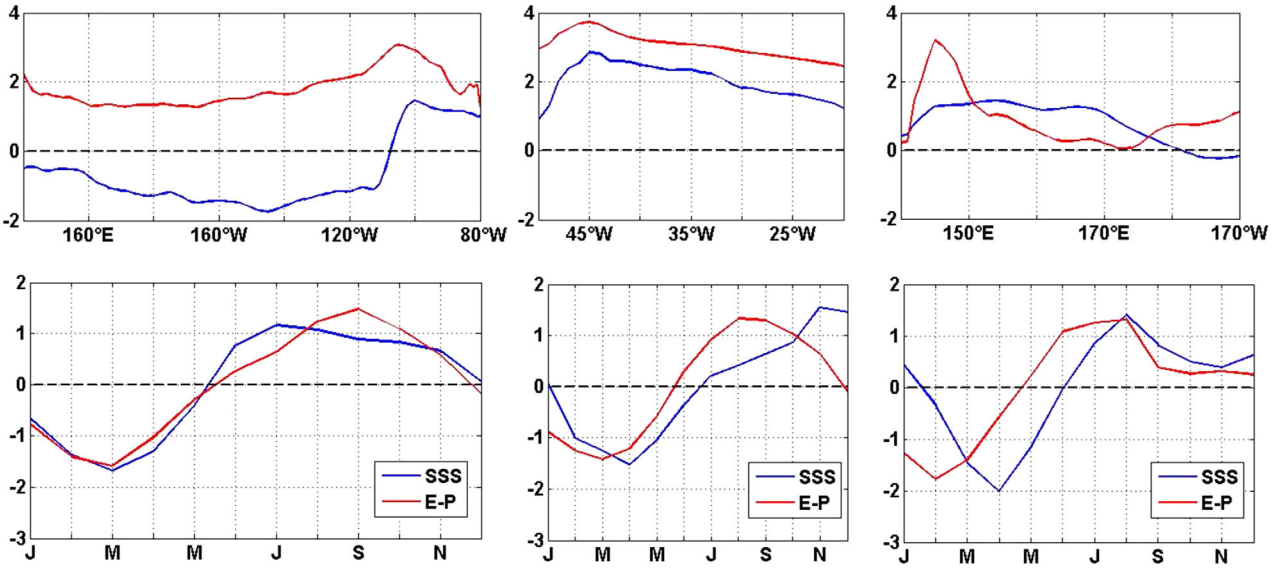

Figure 4. (top) Spatial patterns and (bottom) time functions of the first mode seasonal EOF of the latitudes of SSS (in blue) and E-P (in red) minimum values in the so-called (from left to right) Pacific-ITCZ, Atlantic-ITCZ, and Pacific-SPCZ regions. A 5° longitude running mean was applied for clarity. The units are defined so that the product between spatial pattern and time function denotes degree latitude.

rather than by the seasonal migration of the ITCZ and associated rainfall, consistent with former studies [*Johnson et al*., 2002; *Mignot and Frankignoul*, 2004].

3.3. Interannual Variability

The first interannual EOF mode of SSSmin and E-Pmin latitudes portrays generally consistent longitudinal variations in the three analyzed regions (Figure 5, top). The mean interannual range is of the order of 1°–3°, 0.5°, and 4°–6° latitudes in the Pacific and Atlantic ITCZ and Pacific SPCZ, respectively. The E-Pmin and SSSmin EOF time series (Figure 5, bottom) are positively correlated in the Pacific ITCZ (R = 0.73), Atlantic ITCZ (R = 0.70), and Pacific SPCZ (R = 0.91), indicating that interannual displacements are mostly in phase. Moreover, the EOF time series present a good correspondence with the SOI in the Pacific and with the AMD index in the Atlantic (see correlation values in Table 1). In the Pacific, Figure 5 thus indicates an equatorward migration of SSSmin and E-Pmin during El Niño events (negative SOI) and, conversely, a poleward migration during La Niña events (positive SOI), with maximum changes in the central part of the SPCZ. These migrations agree with results derived from analyses of interannual changes in SSS and P values, and ITCZ and SPCZ displacements [*Delcroix*, 1998; *Gouriou and Delcroix*, 2002; *Dai and Wigley*, 2000; *Servain et al*., 1999; *Folland et al*., 2002; *Chen and Lin*, 2005]. The magnitudes of the meridional migrations are approximately proportional to the strength of ENSO in the Pacific SPCZ, which is not strictly the case in the Pacific ITCZ (e.g., in 1992–1994 and 2002–2004). A detailed analysis of P and SSS changes in relation to different ENSO characteristics can be found in *Singh et al*. [2011] and *Vincent et al*. [2011]. In the Atlantic, Figure 5 then reveals a joint poleward migration of SSSmin and E-Pmin during the positive phase of the AMD index, that is when the SST is warmer to the north (30°N–5°N) than to the south (5°N–20°S) of the mean ITCZ position, and vice versa. A joint southward migration of SSSmin and E-Pmin was also reported by *Dessier and Donguy* [1994, Figure 9] for 1985–1986 (note the reversal in the captions of their Figures 8 and 9) (J. R. Donguy, personal communication, 2015), consistent with the 2° southward displacement of the ITCZ reported by *Servain et al*. [2014].

Table 1. Percent of Variance Explained by the First Mode Seasonal EOF, First Mode Interannual EOF of the SSSmin and E-Pmin Latitudes, and Simultaneous and Maximum Correlation Coefficients at Given Lag Between the Interannual Pacific EOF Time Functions and the SOI and the Interannual Atlantic EOF Time Function and the AMD, as Plotted in Figure 5

	Pacific ITCZ	Atlantic ITCZ	Pacific SPCZ
SSSmin	71%, 48%, 0.60, 0.66, 3	80%, 29% 0.68, 0.68, 0	75%, 86% 0.91, 0.91, 1
E-Pmin	91%, 78% 0.59, 0.60, 1	97%, 74% 0.78, 0.78, 0	71%, 77% 0.89, 0.89, 0

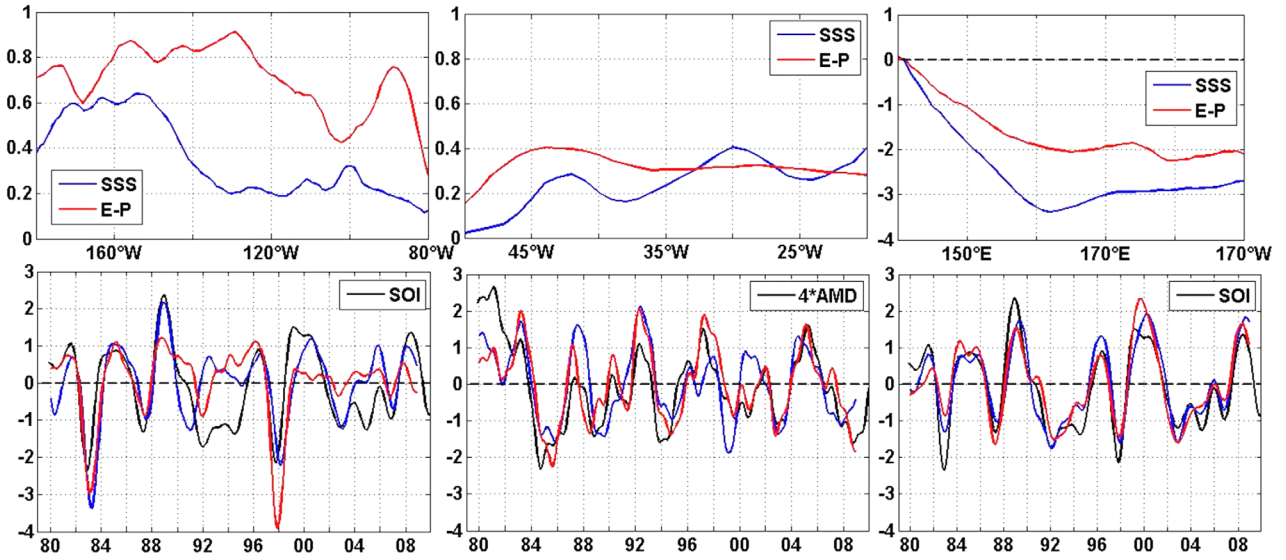

Figure 5. (top) Spatial patterns and (bottom) time functions of the first mode interannual EOF of the latitudes of SSS (in blue) and E-P (in red) minimum values in the so-called (from left to right) Pacific-ITCZ, Atlantic-ITCZ, and Pacific-SPCZ regions. A 5° longitude running mean was applied for clarity. Overplotted as a dark line in the EOF time functions are the SOI in the Pacific ITCZ and SPCZ and the AMD multiplied by four in the Atlantic ITCZ. Note the different vertical scale in the space function of the Pacific SPCZ figure. Units are as in Figure 4.

Taken together, these results show the tendency for the Atlantic ITCZ rainfall and associated SSSmin to migrate toward warmer regions at interannual time scales, as observed at the seasonal time scale.

3.4. Long-Term Trends

The zonal distribution of the long-term (1979–2009) trends of E-Pmin and SSSmin latitudes is shown in Figure 6. There is a general tendency for poleward displacements of E-Pmin for the three analyzed regions, with zonally averaged values of +0.5, +0.4, and −1.6° latitudes for the Pacific ITCZ, Atlantic ITCZ, and Pacific SPCZ, respectively. Figure 6 also underlines that the maximum relative changes appear in the western half of the Atlantic ITCZ and eastern part of the Pacific SPCZ enhancing the diagonal orientations of these convergence zones. The lack of significant long-term trend for the E-Pmin latitudes in the eastern half of the Atlantic corroborates the lack of 1964–2012 long-term ITCZ displacements found at 30°W by *Servain et al*. [2014].

Trends for the latitudes of SSSmin are not as zonally consistent for the Atlantic or for the Pacific ITCZ. Zonally averaged values are close to zero with the alternation of northward and southward displacements. In contrast, there are consistent southward displacements in the trend of the latitudes of SSSmin in the SPCZ (with zonally averaged value of −1.5° latitude) which almost parallel those of E-Pmin. This finding is in agreement with *Hasson et al.*'s [2013a] results which show a low-frequency westward displacement of the high-salinity tongue of the south-eastern tropical Pacific.

To search for possible explanations, we looked at the long-term SST and zonal wind trends computed over the same time period. The mapped SST trend (Figure 7a) shows an indication for a greater warming to the north than to the south of the mean position of the E-Pmin values underneath the Atlantic and Pacific ITCZ (with a maximum warming trend in the West), and a greater warming to the south than to the north of the mean position of the E-Pmin values underneath the SPCZ. From this SST trend map, it is tempting to conclude that the poleward displacements of the latitudes of E-Pmin owe their existence to N-S warming trends. This is in agreement with the positive correlation between P and SST anomalies caused by the convergence zones moving toward warming regions [*Adler et al*., 2008; *Schneider et al*., 2014].

Values of zonal wind trends are shown in Figure 7b. They are similar to those of previous works based on different wind products and slightly different periods [e.g., *England et al*., 2014]. Most of all, they indicate an intensification of the trade winds in the western-central part of the equatorial Pacific. This is reminiscent of a La Nina-type situation (and this also applies for the cold SST trend observed in the eastern-central equatorial Pacific, Figure 7a) that would favor poleward displacements of both SSSmin and E-Pmin in the Pacific (Figure 6). Looking

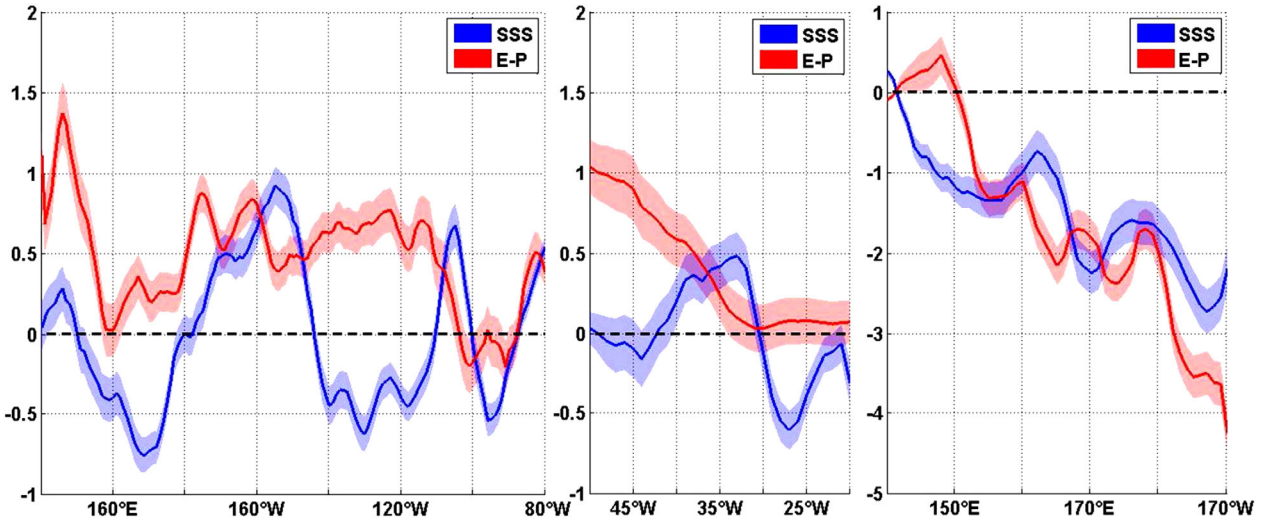

Figure 6. Linear trends in the latitudes of SSS (in blue) and E-P (in red) minimum values as a function of longitude in the so-called (from left to right) Pacific-ITCZ, Atlantic-ITCZ, and Pacific-SPCZ regions. Values were computed every degree longitude from monthly time series covering 1979–2009. Positive values denote northward displacements, and vice versa. Units are degrees per 31 years. A 5° longitude running mean was applied for clarity. The blue and red envelopes represent the errors calculated as the square root of the standard deviation divided by the number of values. Note the different vertical scales.

at the mean positions of SSSmin (as plotted in Figure 7b), there is a hint for the negative zonal wind trends (and associated anomalous poleward Ekman transport) to correspond to the poleward trends in the SSSmin latitudes in the western-central Pacific (Figure 6). This possible cause and effect relationship should however be interpreted with caution as it does not seem to apply in other regions. Similar trend analyses performed on the

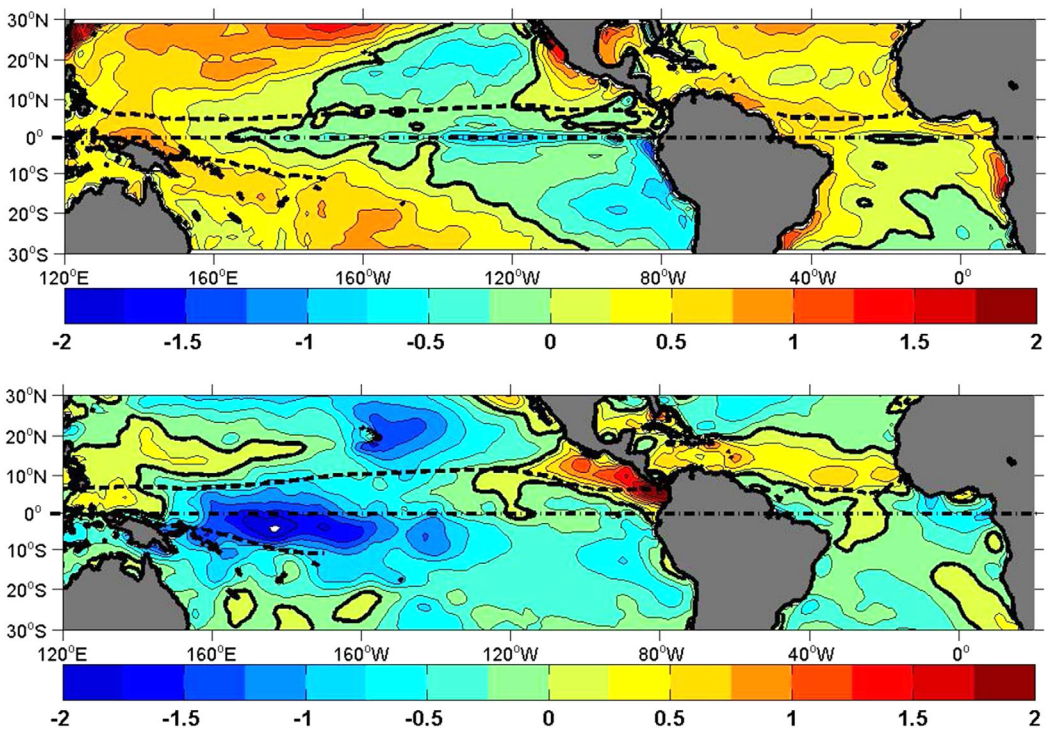

Figure 7. Spatial distribution of the 1979–2009 linear trends in (top) SST and (bottom) zonal surface wind velocity. The heavy black lines are the 0 contours. The heavy black dashed lines denote the position of the (top) E-P and (bottom) SSS minimum values underneath the ITCZ and SPCZ, as in Figure 1. Negative values in the bottom figure represent an increase of the easterly trade winds. Units are °C per 31 years and m/s per 31 years.

spring, summer, fall, and winter seasons only, did not lead to firm conclusions for a possible seasonal enhancement in long-term trends.

4. Conclusion and Discussion

The main goal of the current study was to document the variability in the latitudes of the SSS and E-P minimum zones located underneath the Atlantic and Pacific ITCZ and SPCZ regions, and to clarify their covariability. The idea was also to tentatively improve our knowledge of the ITCZ/SPCZ variability using observed SSS, as the convergence zones, which correspond to the ascending branches of the Hadley circulation, are important components of the climate and global water cycle. Our analysis was conducted from observations collected during 1979–2009, focusing on mean values, seasonal and interannual changes and long-term trends.

The results confirm the existence of a 1°–3° latitude shift between the mean positions of the E-P minima (associated with the ITCZ rain bands within 4°N–10°N) and of the SSS minima in the Atlantic and Pacific oceans. They also reveal that these minima quasi overlap along the diagonally oriented SPCZ. The observed latitudinal mean shifts result from the contribution of poleward Ekman salt transport associated with mean easterly trade wind components. At the seasonal time scale, we showed that the E-P minima migrate poleward in the summer hemispheres, leading the migration of SSS minima by 2–3 months in the Atlantic ITCZ, Pacific SPCZ, and in the eastern part of the Pacific ITCZ. Hence, in these regions, changes in E-P and SSS minima at this time scale are mostly driven by the seasonal migration of convergence zones related to seasonal changes in the sun position. We then confirm the results of *Yu* [2014, 2015], obtained from 2 years of Aquarius data, and contribute additional evidence with 31 years of in situ data that the seasonal displacements of E-P and SSS minima are in antiphase in the central and western parts of the Pacific ITCZ. This peculiarity results from the dominant contribution of Ekman salt transport in the mixed-layer salinity equation, as discussed by this latter author. At the interannual time scale, we demonstrate that the locations of both E-P and SSS minima are affected by ENSO in the Pacific and the AMD in the Atlantic. These minima are displaced by 1°–6° equatorward during El Niño events and poleward during La Niña events in the Pacific. They are also displaced by about 1° poleward during the positive phase of the AMD (and vice versa during the negative phase) in the Atlantic, supporting the idea that the ITCZ tends to move toward the warmer region. Looking at long-term trends (1979–2009), we found poleward displacements of E-P minima (of the order of 50–150 km in 31 years) in the three analyzed regions, a finding which is qualitatively consistent with the differential SST trends computed on each side of the mean position of convergence zones. We also found long-term poleward displacements of SSS minima in the central Pacific ITCZ and in the SPCZ that we tried to relate to the long-term intensification of the trade winds. No clear explanation was obtained to account for the long-term migration of SSS minima in other regions.

The current study was designed to document in a synthetic form, via EOF analysis, the covariability of the E-P and SSS minimum zones and to offer some qualitative hypotheses. In other words, it was not designed to precisely quantify causes for the observed latitudinal displacements. For the SSS minimum zones, for instance, a natural extension of this work would be to analyze the contributions of all the terms of the mixed layer salinity equation, including the contribution of the North and South Equatorial Counter Currents that flow at the latitudes of the ITCZ and SPCZ rain bands (and of the Amazon river discharge in the western tropical Atlantic). This approach has been extensively used in the literature using observations and/or model simulations [*Vialard et al*., 2002; *Bingham et al*., 2010; *Johnson et al*., 2002; *Da-Allada et al*., 2013; *Vinogradova and Ponte*, 2013; *Yu*, 2011; *Hasson et al*., 2013b]. Results from model simulations show that all the terms have to be considered to properly close the salinity budget. However, to our knowledge, this has never been done to quantify changes in the displacements of the SSS minimum zones. Changes in SSS are not necessarily related to changes in the position of the SSS minimum zones. A possibility would be to isolate the term which embodies the area of SSS minimum (e.g., where $\partial S/\partial y = 0$) in the mixed layer salinity equation and then to assess the remaining terms that balance this term.

The long-term poleward displacements of E-P minima associated with the ITCZ and SPCZ suggest a poleward extension of the ascending branch of the Hadley circulation. It would be interesting to test the robustness of this finding with other E-P products, given that large discrepancies are obtained in the spatial patterns of (1979–2010) E-P trends among different E-P products [*Skliris et al*., 2014]. Changes in SSS in the

tropical Atlantic and Pacific also appear at decadal time scales [*Grodsky et al*., 2006; *Cravatte et al*., 2009] and the long-term displacements of SSSmin may thus not be well represented by a linear trend. Similarly, trend estimates are sensitive to the lengths of the SSS data records [e.g., Singh and *Delcroix*, 2011]. Further analysis might hence explore the sensitivity of our trend estimates, based on three decades only, to (at least) decadal variability, as was revealed for the wind stress trend in the Pacific Ocean [*England et al*., 2014]. It would also be interesting to establish the causes of the enhanced obliquity of the SPCZ we observed in the last three decades, whereas a reduced obliquity of the SPCZ is projected in future climate projections [*Brown et al*., 2012; *Cai et al*., 2012]. Further studies clearly need to be carried out to examine more closely the mechanisms responsible for the latitudinal migrations of the SSS and E-P minimum zones, and whether changes in the positions of SSS minima could actually be used as a proxy for the ITCZ and SPCZ migrations.

Acknowledgments

This work is a contribution to the TOSCA/SMOS-Ocean proposal supported by CNES. One of us (M.T.) was supported by an IRD grant. We wish to thank TOTAL S.A. for supporting the ICPMA-UNESCO Chair where a large part of this work was completed. We benefited from numerous data sets made freely available. The Atlantic and Pacific gridded Sea surface salinity data files are made available by the French Sea Surface Salinity Observation Service from http://www.legos.obs-mip.fr/observations/sss/. The OAFlux evaporation product can be downloaded from http://oaflux.whoi.edu. The precipitation GPCP data provided by the NOAA/OAR/ESRL PSD, Boulder, Colorado, USA, can be downloaded from http://www.esrl.noaa.gov/psd/. The TropFlux data are produced under collaboration between LOCEAN/IPSL (Paris, France) and the NIO (Goa, India), and supported by IRD (France). TropFlux relies on data provided by the ECMWF ERA-interim and ISCCP projects. The TropFlux data can be downloaded from http://www.incois.gov.in/tropflux/data.html. The wind data were derived from the ECMWF ERA-interim reanalysis, and can be obtained from: http://www.ecmwf.int/research/era/do/get/era-interim.Comments from anonymous reviewers helped to improve the manuscript.

References

Adler, R. F., et al. (2003), The version 2 Global Precipitation Climatology Project (GPCP) monthly precipitation analysis (1979-Present), *J. Hydrometeorol.*, *4*, 1147–1167.

Adler, R. F., G. Gu, J.-J. Wang, G. Huffman, S. Curtis, and D. Bolvin (2008), Relationships between global precipitation and surface temperature on interannual and longer timescales (1979–2006), *J. Geophys. Res.*, *113*, D22104, doi:10.1029/2008JD010536.

Bellucci, A., S. Gualdi, and A. Navarra (2010), The double-ITCZ syndrome in coupled general circulation models: The role of large scale vertical circulation regimes, *J. Clim.*, *23*, 1127–1145, doi:10.1175/2009JCLI3002.1.

Bingham, F., G. Foltz, and M. McPhaden (2010), Seasonal cycles of surface layer salinity in the Pacific Ocean, *Ocean Sci.*, *6*(3), 775–787, doi:10.5194/os-6-775-2010.

Boyer, T., and S. Levitus (2002), Harmonic analysis of climatological sea surface salinity, *J. Geophys. Res.*, *107*(C12), 8006, doi:10.1029/2001JC000829.

Bretherton, C., C. Smith, and J. M. Wallace (1992), An intercomparison of methods for finding coupled patterns in climate data, *J. Clim.*, *5*, 541–560.

Brown, J., A. Moise, and R. Colman (2012), The South Pacific Convergence Zone in CMIP5 simulations of historical and future climate, *Clim. Dyn.*, *41*, 2179–2197, doi:10.1007/s00382-012-1591-x.

Cai, W., et al. (2012), More extreme swings of the SPCZ due to greenhouse warming, *Nature*, *488*, 365–369, doi:10.1038/nature11358.

Chen, G., and H. Lin (2005), Impact of El Nino/La Nina on the seasonality of oceanic water vapour: A proposed scheme for determining the ITCZ, *Mon. Weather Rev.*, *133*, 2940–2946.

Citeau, J., J. C. Bergés, and H. Demarcq (1988), The watch of the ITCZ migrations over the tropical Atlantic ocean as an indicator in drought forecast over the Sahelian area, *Trop. Ocean Atmos. Newsl.*, *45*, 1–3.

Cravatte, S., T. Delcroix, D. Zhang, M. McPhaden, and J. Leloup (2009), Observed freshening and warming of the western Pacific Warm Pool, *Clim. Dyn.*, *33*(4), 565–589, doi:10.1007/s00382-009-0526-7.

Da-Allada, C., G. Alory, Y. du Penhoat, E. Kestenare, F. Durand, and N. Hounkonnou (2013), Seasonal mixed-layer salinity balance in the tropical Atlantic Ocean: Mean state and seasonal cycle, *J. Geophys. Res. Oceans*, *118*, 332–345, doi:10.1029/2012JC008357.

Dai, A., and T. M. L. Wigley (2000), Global patterns of ENSO-induced precipitation, *Geophys. Res. Lett.*, *27*(9), 1283–1286.

de Boyer Montegut, C., J. Mignot, A. Lazar, and S. Cravatte (2007), Control of salinity on the mixed layer depth in the world ocean: 1. General description, *J. Geophys. Res.*, *112*, C06011, doi:10.1029/2006JC003953.

Dee, D. P., et al. (2011), The ERA-Interim reanalysis: Configuration and performance of the data assimilation system, *Q. J. R. Meteorol. Soc.*, *137*(656), 553–597.

Delcroix, T. (1998), Observed surface oceanic and atmospheric variability in the Tropical Pacific at seasonal and ENSO time scales: A tentative overview, *J. Geophys. Res.*, *103*(C9), 18,611–18,633.

Delcroix, T., and C. Hénin (1991), Seasonal and interannual variations of sea surface salinity in the tropical Pacific Ocean, *J. Geophys. Res.*, *96*(C12), 22,135–22,150.

Delcroix, T., and R. Murtugudde (2002), Sea surface salinity changes in the East China Sea during 1997–2001: Influence of the Yangtze river, *J. Geophys. Res.*, *107*(C12), 8008, doi:10.1029/2001JC000893.

Delcroix, T., M. McPhaden, A. Dessier, and Y. Gouriou (2005), Time and space scales for sea surface salinity in the tropical oceans, *Deep Sea Res., Part I*, *52*(5), 787–813, doi:10.1016/j.dsr.2004.11.012.

Delcroix, T., S. Cravatte, and M. McPhaden (2007), Decadal variations and trends in tropical Pacific sea surface salinity since 1970, *J. Geophys. Res.*, *112*, C03012, doi:10.1029/2006JC003801.

Delcroix, T., G. Alory, S. Cravatte, T. Correge, and M. J. McPhaden (2011), A gridded sea surface salinity data set for the tropical Pacific with sample applications (1950–2008), *Deep Sea Res., Part I*, *58*(1), 38–48, doi:10.1016/j.dsr.2010.11.002.

Dessier, A., and J. R. Donguy (1994), The sea surface salinity in the tropical Atlantic between 10°S and 30°N—Seasonal and interannual variations (1977–1989), *Deep Sea Res., Part I*, *41*(1), 81–100.

Durack, P. J., and S. E. Wijffels (2010), Fifty-year trends in global ocean salinities and their relationship to broad-scale warming, *J. Clim.*, *23*(16), 4342–4362, doi:10.1175/2010JCLI3377.1.

England, M., S. McGregor, P. Spence, G. A. Meehl, A. Timmermann, W. Cai, A. S. Gupta, M. J. McPhaden, A. Purich, and A. Santoso (2014), Recent intensification of wind-driven circulation in the Pacific and the ongoing warming hiatus, *Nat. Clim. Change*, *4*, 222–227, doi:10.1038/nclimate2106.

Folland, C., K. Renwick, J. Salinger, and M. Mullan (2002), Relative influence of the IPO and ENSO on the SPCZ, *Geophys. Res., Lett.*, *29*(13), 1643, doi:10.1029/2001GL014201.

Foltz, G., C. Schmid, and R. Lumpkin (2015), Transport of surface freshwater from the equatorial to the subtropical North Atlantic Ocean, *J. Phys. Oceanogr.*, *45*, 1086–1102, doi:10.1175/JPO-D-14-0189.1.

GCOS (2004), Implementation Plan for the Global Observing System for Climate in Support of the UNFCCC, Executive Summary, October, GCOS-92 (ES), WMO/TD No. 1244, 29 pp. [Available at http://www.wmo.int/pages/prog/gcos/.]

Gouriou, Y., and T. Delcroix (2002), Seasonal and ENSO variations of sea surface salinity and temperature in the South Pacific Convergence Zone during 1976–2000, *J. Geophys. Res.*, *107*(C12), 8011, doi:10.1029/2001JC000830.

Grodsky, S., J. Carton, and F. Bingham (2006), Low frequency variation of sea surface salinity in the tropical Atlantic, *Geophys. Res. Lett.*, *33*, L14604, doi:10.1029/2006GL026426.
Grodsky, S., J. Carton, and F. Bryan (2014), A curious local salinity maximum in the northwestern tropical Atlantic, *J. Geophys. Res. Oceans*, *119*, 484–495, doi:10.1002/2013JC009450.
Hasson, A., T. Delcroix, and J. Boutin (2013a), Formation and variability of the south Pacific sea surface salinity maximum in recent decades, *J. Geophys. Res. Oceans*, *118*, 1–8, doi:10.1002/jgrc.20367.
Hasson, A. E. A., T. Delcroix, and R. Dussin (2013b), An assessment of the mixed layer salinity budget in the tropical Pacific Ocean, Observations and modelling (1990–2009), *Ocean Dyn.*, *63*(2–3), 179–194, doi:10.1007/s10236-013-0596-2.
Held, I. M., and B. J. Soden (2006), Robust responses of the hydrological cycle to global warming, *J. Clim.*, *19*(21), 5686–5699, doi:10.1175/JCLI3990.1.
Hires, R. I., and R. B. Montgomery (1972), Navifacial temperature and salinity along the track from Samoa to Hawaii, 1957–1965, *J. Mar. Res.*, *30*, 177–200.
Johnson, E., G. Lagerloef, J. Gunn, and F. Bonjean (2002), Surface salinity advection in the tropical oceans compared with atmospheric freshwater forcing: A trial balance, *J. Geophys. Res.*, *107*(C12), 8014, doi:10.1029/2001JC001122.
Kao, H.-Y., and G. Lagerloef (2014), Salinity fronts in the tropical Pacific Ocean, *J. Geophys. Res. Oceans*, *120*, 1096–1106, doi:10.1002/2014JC010114.
Lagerloef, G., et al. (2010), Resolving the global surface salinity field and variations by blending satellite and in situ observations, in *Proceedings of the "OceanObs'09: Sustained Ocean Observations and Information for Society" Conference*, vol. 2, edited by J. Hall, D. E. Harrison, and D. Stammer, Eur. Space Agency Publ., Venice, Italy, 21–15 September 2009.
Le Bec, N., A. Juillet-Leclerc, T. Correge, D. Blamart, and T. Delcroix (2000), A coral δ18O record of ENSO driven sea surface salinity variability in Fiji (South—Western Tropical Pacific), *Geophys. Res. Lett.*, *27*(23), 3897–3900.
Lee, T., G. Lagerloef, M. Gierach, H.-Y. Kao, S. Yueh, and K. Dohan (2012), Aquarius reveals salinity structure of tropical instability waves, *Geophys. Res. Lett.*, *39*, L12610, doi:10.1029/2012GL052232.
Lee, T., G. Lagerloef, H.-Y. Kao, M. McPhaden, and J. Willis (2014), The influence of salinity on tropical Atlantic instability waves, *J. Geophys. Res. Oceans*, *119*, 8375–8394, doi:10.1002/2014JC010100.
Levitus, S. (1986), Annual cycle of salinity and salt storage in the world ocean, *J. Phys. Oceanogr.*, *16*(2), 322–343, doi:10.1175/1520-0485.
Maes, C., K. Ando, T. Delcroix, W. Kessler, M. McPhaden, and D. Roemmich (2006), Observed correlation of surface salinity, temperature and barrier layer at the eastern edge of the western Pacific warm pool, *Geophys. Res. Lett.*, *33*, L06601, doi:10.1029/2005GL024772.
Mignot, J., and C. Frankignoul (2004), Interannual to interdecadal variability of sea surface salinity in the Atlantic and its link to the atmosphere in a coupled model, *J. Geophys. Res.*, *109*, C04005, doi:10.1029/2003JC002005.
North, G., T. Bell, R. Cahalan, and F. J. Moeng (1982), Sampling errors in the estimation of the empirical orthogonal functions, *Mon. Weather Rev.*, *110*, 699–706.
Praveen Kumar, B., J. Vialard, M. Lengaigne, V. S. N. Murty, and M. J. McPhaden (2012), TropFlux: Air-sea fluxes for the global tropical oceans—Description and evaluation, *Clim. Dyn.*, *38*, 1521–1543, doi:10.1007/s00382-011-1115-0.
Reverdin, G., E. Kestenare, C. Frankignoul, and T. Delcroix (2007), Surface salinity in the Atlantic Ocean (30°S-50°N), *Prog. Oceanogr.*, *73*, 311–340, doi:10.1016/j.pocean.2006.11.004.
Schanze, J., R. Schmitt and L. Yu (2010), The global oceanic freshwater cycle: A state-of-the-art quantification, *J. Mar. Res.*, *68*, 569–595.
Schneider, T., T. Bischoff, and G. Haug (2014), Migrations and dynamics of the intertropical convergence zones, *Nature*, *513*, 45–53, doi:10.1038/nature13636.
Servain, J., I. Wainer, J. McCreary, and A. Dessier (1999), Relationship between the equatorial and meridional modes of climatic variability in the tropical Atlantic, *Geophys. Res. Lett.*, *26*(4), 485–488.
Servain, J., G. Caniaux, Y. Kouadio, M. McPhaden, and M. Araujo (2014), Recent climatic trends in the tropical Atlantic, *Clim. Dyn.*, *43*(11), 3071–3089, doi:10.1007/s00382-014-2168-7.
Singh, A., and T. Delcroix (2011), Estimating the effects of ENSO upon the observed freshening trends of the western Tropical Pacific Ocean, *Geophys. Res. Lett.*, *38*, L21607, doi:10.1029/2011GL049636.
Singh, A., T. Delcroix, and S. Cravatte (2011), Contrasting the flavors of El Nino-Southern Oscillation using sea surface salinity observations, *J. Geophys. Res. Oceans*, *116*, C06016, doi:10.1029/2010JC006862.
Skliris, N., R. Marsch, S. Josey, S. Good, C. Liu, and R. Allan (2014), Salinity changes in the World Ocean since 1950 in relation to changing surface freshwater fluxes, *Clim. Dyn.*, *43*(3–4), 709–736, doi:10.1007/s00382-014-2131-7.
Sultan, B., and S. Janicot (2000), Abrupt shift of the ITCZ over West Africa and intra-seasonal variability, *Geophys. Res. Lett.*, *27*(20), 3353–3356.
Tanguy, Y., S. Arnault, and P. Lattes (2010) Isothermal, mixed, and barrier layers in the subtropical and tropical Atlantic Ocean during the ARAMIS experiment, *Deep Sea Res., Part I*, *57*, 501–517, doi.10.1016/j.dsr.2009.12.012.
Terray, L., L. Corre, S. Cravatte, T. Delcroix, G. Reverdin, and A. Ribes (2012), Near-surface salinity as nature's rain gauge to detect human influence on the tropical water cycle, *J. Clim.*, *25*(3), 958–977, doi:10.1175/JCLI-D-10-05025.1.
Tian, Y., and C. D. Peters-Lidard (2010), A global map of uncertainties in satellite-based precipitation measurements, *Geophys. Res. Lett.*, *37*, L24407, doi:10.1029/2010GL046008.
Vialard, J., P. Delecluse, and C. Menkes (2002), A modeling study of salinity variability and its effects in the tropical Pacific Ocean during the 1993–1999 period, *J. Geophys. Res.*, *107*(C12), 8005, doi:10.1029/2000JC000758.
Vincent, E., M. Lengaigne, C. Menkes, N. Jourdain, P. Marchesiello, and G. Madec (2011), Interannual variability of the South Pacific Convergence Zone and implications for tropical cyclone genesis, *Clim. Dyn.*, *36*, 1–16, doi:10.1007/s00382-009-0716-3.
Vinogradova, N., and R. Ponte (2013), Clarifying the link between surface salinity and freshwater fluxes on monthly to interannual time scales, *J.Geophys. Res. Oceans*, *118*, 1–12, doi:10.1002/jgrc.20200.
Waliser, D., and C. Gautier (1993), A satellite-derived climatology of the ITCZ, *J. Clim.*, *6*, 2162–2174.
Xie, P., and P. Arkin (1997), Global precipitation: A 17-year monthly analysis based on gauge observations, satellite estimates, and numerical model outputs, *Bull. Am. Meteorol. Soc.*, *78*, 2539–2558.
Yu, L. (2011), A global relationship between the ocean water cycle and near-surface salinity, *J. Geophys. Res.*, *116*, C10025, doi:10.1029/2010JC006937.
Yu, L. (2014), Coherent evidence from Aquarius and Argo for the existence of a shallow low-salinity convergence zone beneath the Pacific ITCZ, *J. Geophys. Res. Oceans*, *119*, 7625–7644, doi:10.1002/2014JC010030.
Yu, L. (2015), Sea surface salinity fronts and associated salinity minimum zones in the Tropical Ocean, *J. Geophys. Res. Oceans*, doi:10.1002/2015JC010790, in press.
Yu, L., and R. A. Weller (2007), Objectively Analyzed air-sea heat Fluxes for the global ice-free oceans (1981–2005), *Bull. Am. Meteorol. Soc.*, *88*, 527–539.